Spatial structure of bivalves in a sandflat: Scale and generating processes

P. Legendre[b,*], S.F. Thrush[a], V.J. Cummings[a], P.K. Dayton[c], J. Grant[d],
J.E. Hewitt[a], A.H. Hines[e], B.H. McArdle[f], R.D. Pridmore[a], D.C. Schneider[g],
S.J. Turner[a], R.B. Whitlatch[h], M.R. Wilkinson[a]

[a]*National Institute of Water and Atmospheric Research, PO Box 11-115, Hamilton, New Zealand*
[b]*Département de sciences biologiques, Université de Montréal, C.P. 6128, succ. Centre-ville, Montréal,
Québec H3C 3J7, Canada*
[c]*Scripps Institution of Oceanography, UC-SD, La Jolla, CA 92093-0201, USA*
[d]*Department of Oceanography, Dalhousie University, Halifax, Nova Scotia B3H 4J1, Canada*
[e]*Smithsonian Environmental Research Center, P.O. Box 28, Edgewater, MD 21037, USA*
[f]*Biostatistics Unit, School of Biological Sciences, University of Auckland, Private Bag, Auckland,
New Zealand*
[g]*Ocean Sciences Centre, Memorial University, St. John's, Newfoundland A1C 5S7, Canada*
[h]*Department of Marine Science, University of Connecticut, Avery Point, Groton, CT 06340-6097, USA*

Abstract

A survey was conducted during the summer of 1994 within a fairly homogeneous 12.5 ha area
of sandflat off Wiroa Island, in Manukau Harbour, New Zealand, to identify factors controlling the
spatial distributions of the two dominant bivalves, *Macomona liliana* Iredale and *Austrovenus
stutchburyi* (Gray), and to look for evidence of adult–juvenile interactions within and between
species. Most of the large–scale spatial structure detected in the bivalve count variables (two
species, several size classes of each) was explained by the physical and biological variables. The
results of principal component analysis and spatial regression modelling suggest that different
factors are controlling the spatial distributions of adults and juveniles. Larger size classes of both
species displayed significant spatial structure, with physical variables explaining some but not all
of this variation. Smaller organisms were less strongly spatially structured, with virtually all of the
structure explained by physical variables. The physical variables important in the regression
models differed among size classes of a species and between species. Extreme size classes (largest
and smallest) were best explained by the models; physical variables explained from 10% to about
70% of the variation across the study site. Significant residual spatial variability was detected in
the larger bivalves at the scale of the study site. The unexplained variability (20 to 90%) found in
the models is likely to correspond to phenomena operating at smaller scales. Finally, we found no
support for adult–juvenile interactions at the scale of our study site, given our sampling scale,
after controlling for the effects of the available physical variables. This is in contrast to significant

---

*Corresponding author. Tel.: (514) 343-7591; fax (514) 343-2293; e-mail: Legendre@ere.umontreal.ca

adult–juvenile interactions found in smaller–scale surveys and in field experiments. Our perception of adult–juvenile interactions thus depends on the scale of study. © 1997 Elsevier Science B.V.

1. Introduction

Scale is emerging as one of the critical factors in ecology because our perception of most ecological variables and processes depends upon the scale at which variables are measured. A conclusion obtained at one scale may not be valid at another scale without sufficient knowledge of scaling effects; this is a source of misinterpretation for many ecological problems (Schneider, 1994). Ecology must deal with scale because organisms and types of environment are rarely homogeneous. Heterogeneity makes ecological variables and processes scale-dependent. Environmental forcing, population and community dynamics, and chance events, are all sources of heterogeneity (Dutilleul and Legendre, 1993) which contribute to create spatial structures of various kinds, such as gradients or density-scapes with mountains of high density and valleys of low density (Schneider, 1987; Legendre and Fortin, 1989; Borcard and Legendre, 1994). The concept of spatial scale in a sampling design refers to three components: grain, lag and extent (He et al., 1994; Thrush et al., 1997b). Since field experiments cannot be conducted at all scales, a good starting point before planning experiments is the identification of the patterns that can be detected at one or several spatial scales.

In this paper, we assess whether the spatial distributions of infaunal bivalves are random or spatially structured. If the distributions appear random, for the spatial grain, lag and extent of the field study, it is unlikely that we will be able to identify relationships indicating processes important in determining distribution patterns. If, however, bivalve distributions do exhibit spatial structure, we can formulate hypotheses about the main determinants of that structure and, by matching the scale of bivalve spatial variation with those of other variables, provide clues of the scale dependence of different processes. Correlative studies do not provide conclusive proof of causal ecological hypotheses, but they may help discard hypotheses for which they provide no support (assuming the test has enough power). They can also help generate hypotheses for future experiments to be conducted at the scale(s) suggested by the results.

We formulated a series of hypotheses, from large to small scale, concerning relationships between bivalve distributions and various factors. Factors may be physical (large-scale processes, with small to large-scale effects), ranging from variations in tidal elevation, wind-wave disturbance and tidal current velocity operating at the scale of the site and beyond, to variation in sediment characteristics around the site (which may also, ultimately, be controlled by hydrodynamics); or biological (predominantly smaller-scale processes) such as interactions between species and different post-settlement life-history stages. The importance of processes may be viewed as corresponding to a gradation in

effects over decreasing scales, with physical effects predominating at large spatial scales, while biological effects predominate at smaller scales. Scale-dependent shifts in the predominance of one process over another (Stommel, 1963; Haury et al., 1978; Amanieu et al., 1989) have also been referred to as hierarchy theory (Allen and Starr, 1982). Care must be taken in applying this term to marine systems, however, because they are open and cannot be described by logical hierarchies. For example, pelagic larvae are not controlled during their development by the local environmental conditions prevailing at the locations where they will eventually settle.

In this paper, we examine the spatial distribution of two bivalves, *Macomona liliana* Iredale, a deposit- and suspension-feeding tellinid, and *Austrovenus stutchburyi* (Gray), a suspension-feeding venerid, within a fairly homogeneous 12.5 ha area of sandflat. In terms of both density and biomass, *Macomona* is the most important species on the Wiroa sandflats. Previous experiments indicate that *Macomona* plays an important role in macrofaunal community dynamics (Thrush et al., 1992, 1996) and is an important food source for eagle rays and waders (Thrush et al., 1994; Cummings et al., 1997; Hines et al., 1997). We were concerned with determining *within* rather than *between* habitat variation. However, the site incorporated sufficient small-scale variation in physical features to be representative of the extensive mid-intertidal sandflat habitat of the region. The extent of the study area and sampling strategy were determined after a pilot study which examined the spatial scales at which bivalve variability was found in this habitat (Hewitt et al., 1997). Spatial modelling was used to describe the significant spatial structures exhibited by *Macomona* and *Austrovenus*, assess the consistency of spatial structures for different size classes, relate patterns to physical factors, and look for intra- and interspecific relationships between bivalves.

2. Materials and methods

2.1. Study site

A 250 m × 500 m area (12.5 ha) was selected on the sandflat of Wiroa Island, Manukau Harbour, New Zealand (37° 01′ S, 174° 49′ E; Fig. 1(a)). A general description of the area and of its physical characteristics is given in Thrush et al. (1997b) and Bell et al. (1997).

The area was marked off into 200 grid cells of 25 m × 25 m each. One sampling station was selected at random within each cell (with the help of a pseudo-random number generator) and marked by a peg (Fig. 1(b)). The sampling ''grain'' was a plot of 50 cm × 50 cm, 15 cm deep, for large bivalves, and three 13 cm diameter × 15 cm deep cores for smaller animals. Grain was different again for physical variables, varying from a point for elevation and for variables derived by modelling, to the cores described above for sediment composition. The resulting lag (distance between sample centres) ranged from 5 to 530 m, with a mean distance of 201 m among all pairs of locations, and a mean distance of 31 m between neighbouring plots.

Sampling was carried out on 22 and 23 January 1994 at the 200 locations described above. On 16 February 1994, new 0.25 m^2 plots were dug out at 31 of the 200 locations
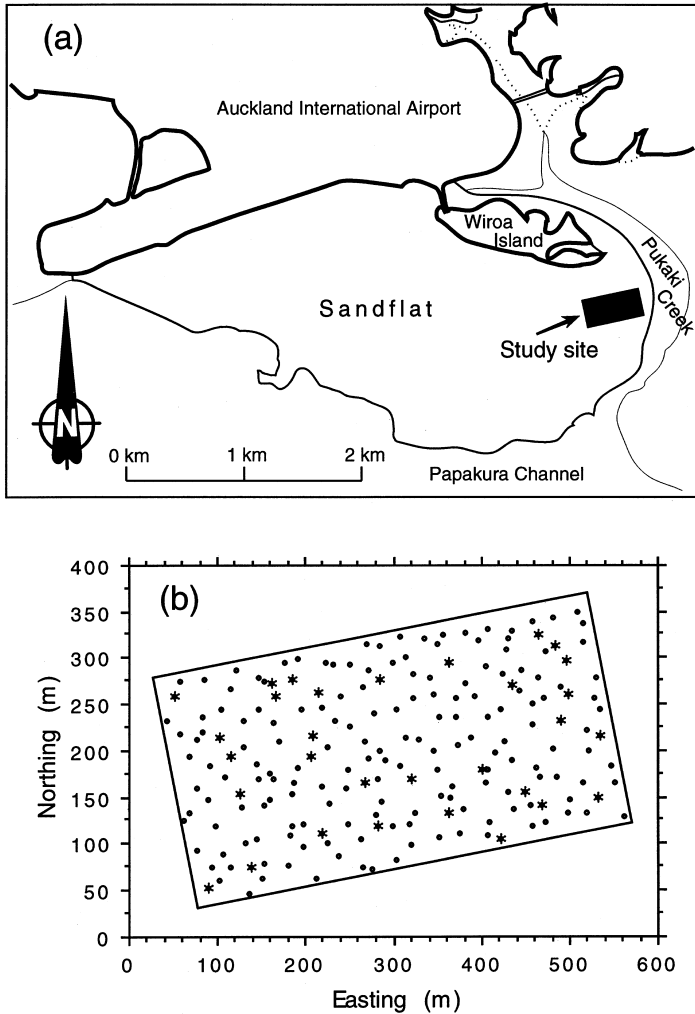
Fig. 1. (a) Position of the study site on the Wiroa Island sandflat. (b) Location of the 200 sampling stations in the study site, including the 31 stations sampled on 16 February (stars). Coordinates are from an arbitrary zero mark.

(Fig. 1(b), stars); the rationale through which these 31 locations have been selected is described in Thrush et al. (1997b). Although tests of significance computed from 31 locations will have lower power than with 200 locations, this information allowed us to assess the short-term persistence of patterns.

For each location, three cores totalling 0.04 m^2 were taken and the remaining sediment in the 0.25 m^2 quadrat was excavated to a depth of 15 cm. Sediment collected in corers was sieved (500 μm mesh) to extract macrofauna, while the remaining

sediment excavated from the quadrat was sieved (4 mm mesh) to collect large *Macomona liliana* and *Austrovenus stutchburyi*.

2.2. Bivalve count data

For the 22 January data, numbers of *Macomona* > 15 mm and *Austrovenus* > 10 mm are based on the total from three core samples and the remaining sediment excavated from the 0.25 m^2 quadrats. Numbers of smaller individuals (*Macomona* 4–15 mm, *Macomona* 2.5–4 mm, *Macomona* 0.5–2.5 mm, *Austrovenus* 4–10 mm, *Austrovenus* 2.5–4 mm, and *Austrovenus* 0.5–2.5 mm) are based on the three core samples only. Data were available for 199 of the 200 triplicate core samples only. Data for the missing sample location were estimated by regression for animals larger than 4 mm, as counts for quadrats and cores were well correlated for the larger size classes. The 200 core samples collected in January produced only 17 *Austrovenus* (4–10 mm), for an estimated mean density of 2.1 animals · m^{-2}; this variable was not analysed.

On 16 February 1994, the bivalves were counted from 31, 0.25 m^2 quadrats, in the following categories: *Macomona* > 15 mm, *Macomona* 4–15 mm, *Austrovenus* > 10 mm, and *Austrovenus* 4–10 mm. This gave us a total of 11 usable bivalve counts: 7 for 22 January and 4 for 16 February. All counts were log-transformed prior to the analyses ($\ln(x + 1)$). This transformation was enough to normalise the counts of *Macomona* > 4 mm and to make all other counts far more symmetrical than the raw data.

2.3. Physical variables

To relate spatial structure in the distribution of *Macomona* and *Austrovenus* to various habitat features, data on a variety of physical variables were collected coincident with bivalve sampling, with further information on physical processes interpolated from hydrodynamic models and field measurements (Bell et al., 1997). A major difficulty was the large number of potentially important controlling variables; in such situations, choices inevitably have to be made prior to sampling. Our choices were guided by two weeks of intensive discussions that took place among the authors of this paper and other invited scientists, during a workshop organised by the National Institute of Water and Atmospheric Research of New Zealand (NIWA) in Hamilton, NZ, prior to the sampling campaign itself.

2.3.1. Sediment characteristics
Shell hash (i.e. broken bivalve shell) was measured, at 185 stations, as the dry mass (g) of broken bivalve shell sieved (500 mm mesh) from the three sediment cores. Shell hash in our study area was mainly in a layer buried about 3–7 cm below the sediment surface. Values vary from 5 to 157 g per set of three cores. The shell hash variable was normalised by the square root transformation. Negative relationships between the shell hash and adult *Macomona* could relate to difficulties in moving, and extending siphons through a shell hash layer. Apparent shell hash effects could also be explained by covariation with hydrodynamic variables or with elevation.

Data on sediment grain size characteristics (% gravel, % sand and % mud) were

gathered at 22 locations; only four of these were resampled in February. The study area is mainly fine sand (98.7%; Thrush et al., 1997b) and previous sampling indicated very little variation in sediment grain size within the area used for this study (Thrush et al., 1994). Most if not all the material classified as ''gravel'' for particle size was actually shell hash.

2.3.2. Elevation

Elevation and position were measured at the 200 grid locations using a geodimeter. Bed elevation varied by 1.3 m across the 200 sampling stations (from 1.95 to 3.26 m above chart datum). Elevation is a potentially important variable describing sandflat topography; it is likely to reflect large-scale zonation patterns.

2.3.3. Hydrodynamics

Hydrodynamic variables are likely to be important determinants of bivalve distributions influencing larval deposition (Luckenbach, 1984; Butman, 1987; Snelgrove, 1994), the transport of recently settled juveniles (Cummings et al., 1993; Commito et al., 1995a,b; Roegner et al., 1995), food supply (Emerson and Grant, 1992), and feeding behaviour (Ertman and Jumars, 1988; Monismith et al., 1990; O'Riordan et al., 1993). As an important determinant of sediment grain size characteristics, hydrodynamic forces are likely to covary with sediment variables (Snelgrove and Butman, 1994). The variables that were available to the present study were derived from numerical model simulations for tidal currents and wind-waves, described by Bell et al. (1997). Two predictions can be made about physical–biological interactions: (1) more juveniles should be found where bed shear stress and wave action are lower; (2) regions of higher bed shear stress and wave action may be preferred by adults, because physical energy may maximise the supply of food.

Waves and currents both generate shear stress at the sediment surface (Grant and Madsen, 1979), but for convenience we treat the two processes separately. The drag force exerted upon water moving over the sea bed demands that the moving fluid impart some of its momentum to the seabed. At the sediment interface, the transfer of momentum (i.e. shear stress) is a maximum, and in turbulent flows it is proportional to the square of the time-averaged fluid velocity (U^2), with the stress equal to $\rho C_x U^2$ (where C_x is the drag coefficient and ρ is seawater density). For tidal currents, bed shear stresses ($N \cdot m^{-2}$) under peak ebb- and flood-tide velocities, during a mean tide, correspond to shearing forces applied per unit area; they were computed from the depth-averaged tidal hydrodynamic model for a mean tide. A further variable was computed in the form of rate of energy dissipation per unit area at the bed, or the power expended per unit area (proportional to U^3); it is measured in $kg \cdot s^{-3}$. Both variables have been multiplied by 1000 for convenience. While the distributions of the peak ebb tide variables were fairly normal-looking, this is not the case for the peak flood tide variables (shear stress and rate of energy dissipation) that were skewed positively; a log transformation solved this problem ($\ln(x)$).

Wind-waves also disturb the sandflat and generate sediment transport. For waves, the rate of energy dissipation has been integrated over time during a tidal cycle when the bed was inundated, to give work done per unit area of bed ($kg \cdot s^{-2}$). The drag

coefficient is typically an order of magnitude higher under waves than for tidal currents. Values were calculated based on model simulations of peak wave orbital velocities at the bed condensed to a single scenario of a 0.3 m wave height (exceeded only 20% of the time at this site for onshore winds ≥ 17 knots) and a typical mean period of 2.7 s. This was done for the two most common wave directions, SW and WSW (Bell et al., 1997). The percentage of time each station of the grid is covered by spring and neap tides was also computed, as well as the percentage of time the waves stir the plot during spring and neap tides (R.A. Walters, pers. comm.). All these variables are strongly and negatively correlated with elevation, as expected.

Only some of the physical variables were included in the regression analyses. Among the 22 physical variables mentioned above, many are likely to be highly correlated. For each group of physical variables, those that were more strongly correlated with bivalve counts were selected for inclusion in statistical modelling. Preventing different but correlated variables from becoming significant in different models makes the comparison of models easier. The pre-selection procedure presents the same problems as forward selection of explanatory variables prior to modelling. Hopefully, this risk will be counterbalanced by a gain in clarity of the models. The alternative would have been to resort to ridge regression to deal with high collinearities; this methods presents problems of its own (Legendre and Legendre, 1997).

1. Six highly collinear ''water cover'' variables were available. The ''percent of time the plot is covered by more than 20 cm water during spring tide'' had the largest sum of correlations with the other five, as well as the largest correlations (when significant) with all the bivalve count variables. This variable is biologically reasonable, reflecting the time when food particles are put into motion by wave activity. This variable only was used in the statistical model.
2. Three highly collinear ''wave stirring'' variables were available. Among them, the ''percent of time large waves stir the plot during spring tide'' had the largest sum of correlations with all the others. It is also strongly collinear with the water cover variable retained in the previous paragraph ($r = 0.953$).
3. Peak ebb shear stress and rate of energy dissipation were very highly correlated ($r = 0.9995$), as were peak flood shear stress and rate of energy dissipation ($r = 0.9999$). Thus, only the shear stress variables, that relate directly to the potential for sediment transport in the absence of waves, were retained in the spatial modelling, in order to reduce collinearity.
4. The work variables (SW and WSW winds) were retained in the spatial modelling. Correlations with the bivalve counts were high.

The preliminary analysis, which started with 22 physical variables, resulted in eight variables that were spatially structured (they all had highly significant trend surface equations: Section 2.4) and significantly related to the bivalve count data. Elevation to the powers 2 and 3 were also included in the modelling effort in order to model nonlinear relationships to bivalve counts. The correlations among the variables to be used in modelling are summarised in Table 1. The large correlations ($r > 0.6$), underscored in that table, indicate that there is still a large amount of collinearity among

Table 1
Pearson correlations among the physical variables retained for spatial modelling of the bivalve count data

	Shell hash	Elevation	Elevation^2	Elevation^3	Ebb stress	Flood stress	SW work	WSW work	>20 cm water	Wave stirring
Shell hash[a]	1.0000	0.3505	0.3404	0.3286	0.2784	−0.4935	0.3842	0.2912	−0.3417	−0.4050
Elevation	0.3505	1.0000	0.9980	0.9926	0.1266	−0.6500	0.9002	0.8985	−0.9992	−0.9556
Elevation^2	0.3404	0.9980	1.0000	0.9983	0.1381	−0.6588	0.8966	0.9211	−0.9997	−0.9547
Elevation^3	0.3286	0.9926	0.9983	1.0000	0.1470	−0.6649	0.8893	0.9392	−0.9966	−0.9495
Ebb stress	0.2784	0.1266	0.1381	0.1470	1.0000	−0.4092	0.0365	0.1975	−0.1309	−0.2235
Flood stress[b]	−0.4935	−0.6500	−0.6588	−0.6649	−0.4092	1.0000	−0.4864	−0.7243	0.6566	0.6084
SW work	0.3842	0.9002	0.8966	0.8893	0.0365	−0.4864	1.0000	0.7795	−0.8966	−0.8782
WSW work	0.2912	0.8985	0.9211	0.9392	0.1975	−0.7243	0.7795	1.0000	−0.9139	−0.8507
>20cm water[c]	−0.3417	−0.9992	−0.9997	−0.9966	−0.1309	0.6566	−0.8966	−0.9139	1.0000	0.9531
Wave stirring[d]	−0.4050	−0.9556	−0.9547	−0.9495	−0.2235	0.6084	−0.8782	−0.8507	0.9531	1.0000

$n = 200$, except in comparisons involving shell hash ($n = 185$). Correlations larger than 0.6 are underscored.

[a] Shell hash: square root transformation. $n = 185$.

[b] Flood shear stress: natural logarithm transformation.

[c] % time the plot is covered by more than 20 cm water during spring tide.

[d] % time large waves stir the plot during spring tide.

these variables; only shell hash and ebb shear stress are fairly linearly independent of the other physical variables. Collinearity was reduced by backward elimination of non-significant variables during regression modelling.

2.3.4. Chemistry

To indicate the availability of food to deposit feeders, data were obtained at 19 stations for percentage of organic carbon and nitrogen in the sediment, using a Perkin–Elmer elemental analyser. Correlations between these variables and log-transformed bivalve counts were in general low. These variables, which are not available for the 200 stations, were not used in the modelling. Surficial sediment chlorophyll concentration was also determined following the methods described in Thrush et al. (1994), but after analysing a random subset, no variation had been detected and the variable was abandoned.

2.4. Statistical methods

A variety of methods have been proposed to investigate spatial autocorrelation, including spectral analysis, spatial autocorrelograms, variograms and other forms of variance–distance curves; these techniques are presented in various textbooks and review papers about spatial statistics and numerical ecology (Sokal and Oden, 1978; Cliff and Ord, 1981; Ripley, 1981; Upton and Fingleton, 1985; Burrough, 1987; Legendre and Fortin, 1989; Isaaks and Srivastava, 1989; Haining, 1990; Legendre and Legendre, 1997). Frequency-based techniques (e.g. spectral analysis) cannot be used for irregularly spaced observations; distance-based techniques (e.g. correlogram analysis) are more appropriate here.

A combination of spatial autocorrelograms, trend surface analysis, and mapping was used to describe spatial structures. Spatial autocorrelograms were computed using Moran's I spatial autocorrelation coefficient; following Oden (1984), an overall test of the significance of each spatial autocorrelogram was performed by checking that the most significant spatial autocorrelation coefficient found in a correlogram was significant at a Bonferroni-corrected significance level $\alpha' = \alpha/k$ where k is the number of autocorrelation coefficients in the correlogram.

Trend surface analysis (Student, 1914) is a regression of a dependent variable y on a polynomial function of the geographic coordinates X and Y of the sampling stations where the variable has been observed or measured. The X and Y coordinates were easting and northing respectively, in km, measured from an arbitrary "zero" surveyor's mark. These coordinates were centred on their respective means in order to reduce the linear dependency (collinearity) between the first and second-degree terms of the spatial polynomial of geographic coordinates; the mean point corresponds roughly to the centre of the study site. The amount of variation explained by a trend surface equation is not changed by a translation of the spatial coordinates across the map. The trend surfaces were computed by ordinary least-squares fitting of a polynomial equation of these centred X's and Y's. The following third-degree polynomial equation was used in the present study, as suggested by Legendre (1990):

$$\hat{y} = b_0 + b_1 X + b_2 Y + b_3 X^2 + b_4 XY + b_5 Y^2 + b_6 X^3 + b_7 X^2 Y + b_8 XY^2 + b_9 Y^3$$

where the *b*'s are the regression coefficients to be estimated by regression. Non-significant terms (called *monomials*) of the spatial polynomial were removed using a backward elimination procedure.

The rationale behind this polynomial is the following. Let us assume some general shape for the biological phenomena to be described; for instance, a phenomenon may start from some mean value of the measured variable, increase in intensity to a maximum, then go down to a minimum, and come back to the mean value. The amount of space required for the phenomenon to complete a full cycle—whatever the shape it may take—is called its scale. Commonly used models for such shapes are sine functions; models for these functions are easy to generate, and several methods exist in the time series literature for fitting them to actual data series. In the present study, we will not restrict allowable phenomena to trigonometric functions; we will try to model instead any phenomenon that has the general behaviour described above (mean, maximum, minimum, and back to the mean) using polynomial functions; these functions are more flexible than sines or cosines, in that they do not require symmetry or strict periodicity. The degree of the polynomial which is appropriate to model an anticipated phenomenon is predictable. For instance, if a variable has spatial variation at the scale of the study site (say, in the X direction = easting), it should be correctly modelled by a polynomial of degree 3, which has two extreme values, a minimum and a maximum. If the scale of the phenomenon is larger than the study site, a polynomial of degree less than 3 should be sufficient; degree 2 if only one maximum, or only one minimum, is observed in the sampling window; and degree 1 if the study site is limited to the increasing, or decreasing, portion of the phenomenon. Conversely, if the scale of the phenomenon controlling the variable is smaller than the study site, more than two extreme values (minima and maxima) should be found in the study site, and a polynomial of order larger than 3 would be required to model it correctly. So, using a polynomial of degree 3 acts as a filter, because it is a way of looking for phenomena that are of the same scale, or larger, than the study site. The same reasoning applies to the X (= easting) and Y (= northing) directions if we use of a polynomial combining the X and Y geographic coordinates.

Correlations among bivalves in different size classes were investigated using principal component analysis. Eigenvalues and eigenvectors were computed from the correlation matrix and the eigenvectors were scaled to the square root of their respective eigenvalues. With this scaling, plots correctly represent the projection angles among variables. Arc cosine transformations of the correlations give the angles between variables in multidimensional space (Legendre and Legendre, 1983). Visually, if lines are drawn from the origin to the points representing different variables, then the angle between two lines represents the correlation between the corresponding variables, a small angle meaning a high correlation.

Spatial modelling was performed using a method derived from that proposed by Borcard et al. (1992) and Borcard and Legendre (1994) to partition the variance of a dependent variable (or set of dependent variables) among environmental and spatial components. Our specific purpose here was to take the spatially-structured variation as a measure of the dependent variables' variation worth explaining, and to measure by how much this fraction had decreased after incorporating different groups of explanatory variables into the models.

2.5. Spatial modelling

Each bivalve count variable was modelled through a process involving five steps. The physical variables were used first to explain the spatial variation of the bivalve counts, followed by the biological variables. For each dependent bivalve count variable, only those size classes that were larger than or equal to that of the modelled variable were used as explanatory variables, following the hypothesis that small animals can only be directly affected by other bivalves of the same or larger sizes (e.g. feeding adults may disturb juveniles but not the converse). Previous studies on this sandflat provided no indication for indirect effects of aggregations of juveniles on adults. Biological interaction variables may also explain part of the small-scale, non-spatially structured variation in the data. When biological interactions were found, we checked whether the variation thus explained was spatial or not.

1. Step 1: Calculate the coefficient of multiple determination (R^2) of the spatially structured variation in the dependent variable.
2. Step 2: Do the multiple regression modelling, selecting from the physical variables described in the previous section.
3. Step 3: Check whether the remaining variation is spatially structured, by adding the nine terms of the spatial polynomial to the multiple regression. The statistic of interest is the increase in explained variation, ΔR^2. When a significant spatial polynomial cannot be found, the ΔR^2 value is given for all nine terms of the spatial polynomial.
4. Step 4: Add the biological interaction variables to the physical equation, if significant. Two statistics are of interest: the total fraction of variation, R^2, explained by the combined action of the physical and biological variables, and the increase in explained variation due to the biological variables alone ΔR^2 (with indication of the significance of that increase).
5. Step 5: If the biology provided significant explanatory variables, does there remain some spatially-structured variation in the residuals? If so, it could correspond to spatial variation not explained by the variables in the model, or to large-scale spatial variation appearing in the residual data after removing local biological effects. The statistic provided, ΔR^2, is the same as in step 3.
6. Summary statistic: total explained variation at the outset of the modelling process (R^2), for significant variables, excluding the variation explained by non-significant spatial polynomials.

3. Results

3.1. Do the distributions of bivalves display significant spatial structures?

3.1.1. Spatial autocorrelograms of bivalve counts
The spatial all-directional autocorrelograms (log-transformed data) for bivalve counts are presented in Fig. 2. All correlograms for 22 January, based upon a large number of observations, were globally significant. In contrast, the correlograms for 16 February
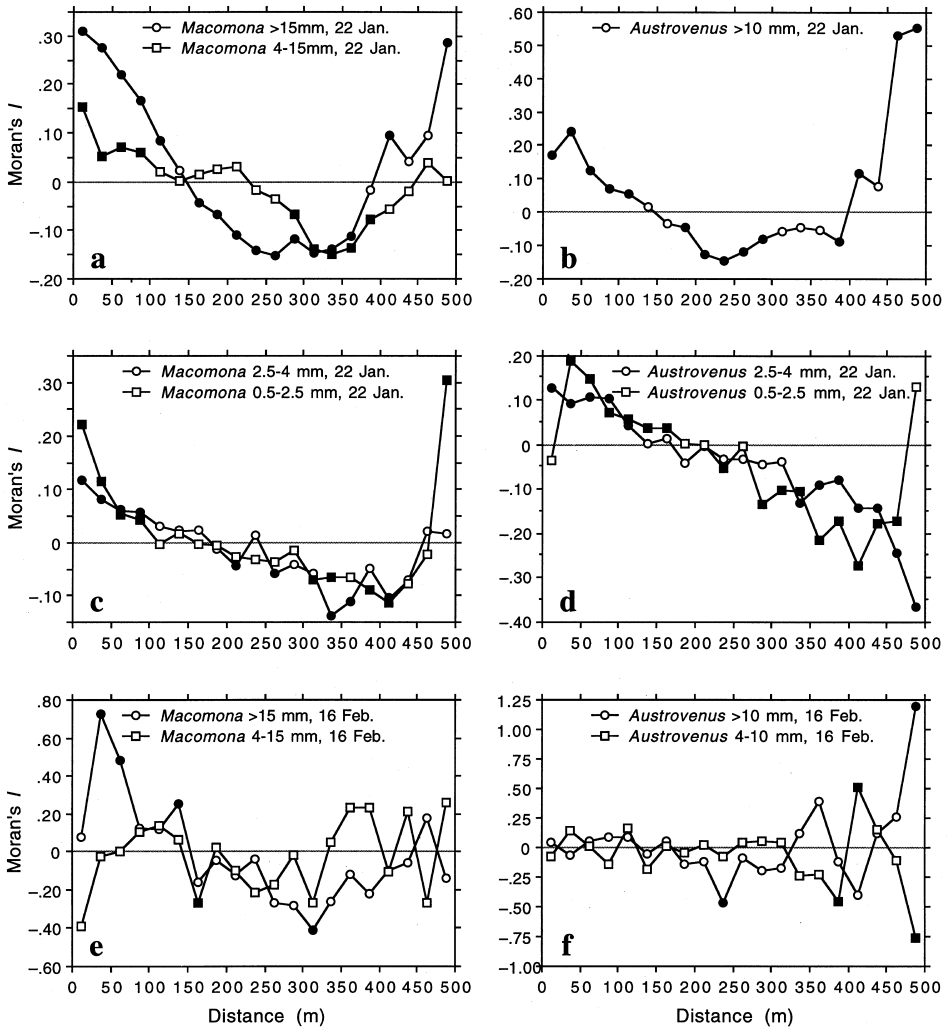
Fig. 2. All-directional spatial autocorrelograms for log-transformed bivalve counts. Graphs (a–d) are based upon 199 or 200 sites sampled on 22 January, while graphs (e–f) are based upon 31 sites sampled on 16 February. Significant values of Moran's I spatial autocorrelation coefficient ($p \leq 0.05$) are represented by black symbols.

were generally not significant, except the one for *Macomona* >15 mm. Lack of significance can be attributed to low power, due to the calculations being based upon only 31 sampling stations. Recomputing these correlograms with 10 distance classes instead of 20 did not lead to more significant results.

Interpretation of the spatial structures represented by the significant correlograms was based on the simulations presented in Legendre and Fortin (1989). Fig. 2(a) and 2(b) correspond to large aggregation structures (shaped as bumps, troughs, or waves) that are

Table 2
Trend surface models for the bivalve count variables $(\ln(x+1))$

● Model for *Macomona* >15 mm, 22 January, counted in 0.25 m^2	
$n=200$, $\Sigma=8003$, $\bar{y}=40.02$, S.E.$=0.791$, dens.$=160.1$	$R^2=0.3171$, $p<0.0001$
$\hat{y}=3.694-1.927\ X+1.722\ Y-7.590\ XY+36.230\ X^3-47.336\ X^2Y$	
● Model for *Macomona* 4–15 mm, 22 January, counted in 0.04 m^2	
$n=200$, $\Sigma=209$, $\bar{y}=1.05$, S.E.$=0.085$, dens.$=26.1$	$R^2=0.1192$, $p<0.0001$
$\hat{y}=0.684+0.671\ X+1.319\ Y-6.161\ X^2$	
● Model for *Macomona* 2.5–4 mm, 22 January, counted in 0.04 m^2	
$n=199$, $\Sigma=139$, $\bar{y}=0.70$, S.E.$=0.080$, dens.$=17.5$	$R^2=0.1094$, $p<0.0001$
$\hat{y}=0.429+0.889\ X-4.288\ X^2+10.135\ XY$	
● Model for *Macomona* 0.5–2.5 mm, 22 January, counted in 0.04 m^2	
$n=199$, $\Sigma=551$, $\bar{y}=2.77$, S.E.$=0.207$, dens.$=69.2$	$R^2=0.1458$, $p<0.0001$
$\hat{y}=1.147+0.924\ X+1.562\ Y-9.212\ X^2+19.395\ XY$	
● Model for *Macomona* >15 mm, 16 February, counted in 0.25 m^2	
$n=31$, $\Sigma=964$, $\bar{y}=31.10$, S.E.$=2.162$, dens.$=124.4$	$R^2=0.3936$, $p=0.0033$
$\hat{y}=3.424-0.939\ X+4.012\ Y-133.062\ X^2Y$	
● Model for *Macomona* 4–15 mm, 16 February, counted in 0.25 m^2	
$n=31$, $\Sigma=202$, $\bar{y}=6.52$, S.E.$=0.753$, dens.$=26.1$	$R^2=0.1503$, $p=0.0312$
$\hat{y}=1.467+15.412\ X^2$	
● Model for *Austrovenus* >10 mm, 22 January, counted in 0.25 m^2	
$n=200$, $\Sigma=374$, $\bar{y}=1.87$, S.E.$=0.291$, dens.$=7.5$	$R^2=0.3483$, $p<0.0001$
$\hat{y}=0.288+1.630\ X+18.088\ X^2-31.653\ XY+23.727\ Y^2-49.721\ X^3+87.807\ X^2Y$	
● Model for *Austrovenus* 2.5–4 mm, 22 January, counted in 0.04 m^2	
$n=199$, $\Sigma=185$, $\bar{y}=0.93$, S.E.$=0.084$, dens.$=23.2$	$R^2=0.1617$, $p<0.0001$
$\hat{y}=0.495-1.210\ X+3.127\ Y-89.791\ X^2Y$	
● Model for *Austrovenus* 0.5–2.5 mm, 22 January, counted in 0.04 m^2	
$n=199$, $\Sigma=192$, $\bar{y}=0.96$, S.E.$=0.095$, dens.$=24.1$	$R^2=0.1694$, $p<0.0001$
$\hat{y}=0.482-1.718\ X+9.415\ XY-67.507\ X^2Y+131.171\ XY^2$	
● Model for *Austrovenus* >10 mm, 16 February, counted in 0.25 m^2	
$n=31$, $\Sigma=72$, $\bar{y}=2.32$, S.E.$=1.131$, dens.$=9.3$	$R^2=0.5508$, $p<0.0001$
$\hat{y}=0.119+27.920\ X^2-40.770\ XY$	
● Model for *Austrovenus* 4–10 mm, 16 February, counted in 0.25 m^2	
$n=31$, $\Sigma=56$, $\bar{y}=1.81$, S.E.$=0.351$, dens.$=7.2$	$R^2=0.2917$, $p=0.0080$
$\hat{y}=0.756+9.493\ Y-702.473\ Y^3$	

X and Y are geographic coordinates in km, centred on their respective means. The fitted value of the dependent variable in each model is designated by $\hat{y}$. R^2 is the coefficient of multiple determination of the model, and p the associated probability. All terms reported in the trend surface equations are significant ($p \leq 0.05$); some regression coefficients are large because the squared and cubic terms of the spatial polynomial are very small numbers. Basic statistics are also provided for the untransformed counts: n is the number of observations; Σ designates the sum of bivalves of the given species and size, counted in all samples; $\bar{y}$ is the mean, and S.E. is the standard error of the mean; dens. is the mean estimated density (animal·m^{-2}).

the same size or larger than the study site; for bumpy or wavy structures, the distance between successive peaks or troughs is twice the distance where the minimum autocorrelation value occurs in the correlogram. Fig. 2(c) and 2(d) correspond to spatial gradients running over the site, that are perhaps part of bumpy or wavy structures that occur on spatial scales larger than our study area. Correlograms cannot be of further help in determining the shapes of these large-scale structures because they exceed the size of the study site. So, their shapes will now be investigated using trend surface analysis and mapping; Figs. 4–7 will help interpret the correlograms.
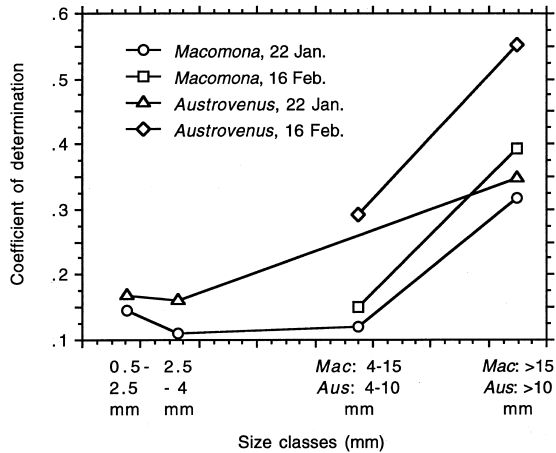
Fig. 3. Coefficients of determination (R^2) of the spatial trend-surface models, where a significant model has been identified. Details in Table 1.

3.1.2. Trend surface analyses

Highly significant trend surface equations were found for all bivalve variables (Table 2). This corroborates the interpretations of the autocorrelograms; the spatial distributions of these organisms are not random, but highly organised at the scale of the 12.5 ha study site. The trend surface models for the smaller animals have much smaller coefficients of determination (10–20%) than for larger animals (30–55%). The best models, that is, the models with the highest coefficients of determination (R^2), are for the *Macomona* > 15 mm and *Austrovenus* > 10 mm (Table 2, Fig. 3). Also, the coefficients of determination are consistently higher for *Austrovenus* than for *Macomona*, despite the fact that *Macomona* were usually far more numerous than *Austrovenus*. That the coefficients of determination are consistently higher for 16 February than for 22 January is due to a large extent to a higher ratio of number of parameters to sample size.

3.1.3. Maps

Maps that illustrate the trend surface equations are presented for the largest and smallest size classes (Fig. 4 Fig. 5 Fig. 6 Fig. 7); the field counts are also presented in each case for comparison. The two species displayed very different spatial patterns for their largest size classes (the correlation of these two variables across 200 locations is low, $r = 0.0481$), although they presented very similar correlograms (Fig. 2 (a–b)); Legendre and Fortin (1989) had already shown that different spatial structures may lead to the same type of correlogram. What the two species had in common is a wavy structure whose main axis of variation is NW to SE. In the same way, while the trend surfaces for the smallest *Macomona* and *Austrovenus* are very different (the correlation of these two variables is $r = 0.2039$), the all-directional correlograms seem to have picked up mostly the main spatial gradient in each of these surfaces (Fig. 2 (c–d)).

(a) *Macomona* > 15 mm counts at the 200 sampling stations

```
35   41   37   48   52   68   64   51   52   19   50   48   46   50   40   33   27   29   32   39

22   47   46   33   51   71   54   71   44   56   63   50   30   49   46   41   43   40   29   32

45   66   58   60   27   59   50   52   41   40   54   39   41   46   47   19   24   30   20   28

41   56   33   60   59   60   53   52   26   39   31   33   29   54   37   18   36   42   27   29

48   36   38   34   41   55   42   67   53   57   34   34   42   33   32   46   33   18   27   32

41   32   41   35   48   52   40   56   40   44   41   43   44   41   43   32   22   34   30   32

17   29   50   67   35   52   28   44   45   28   30   35   30   28   35   37   20   28   50   31

27   43   38   44   29   44   35   39   44   38   40   24   37   43   35   31   38   48   50   37

27   42   36   36   29   46   39   38   29   37   38   35   35   38   25   38   39   54   50   44

52   41   32   41   42   28   47   22   24   17   37   31   38   29   41   38   36   46   38   52
```
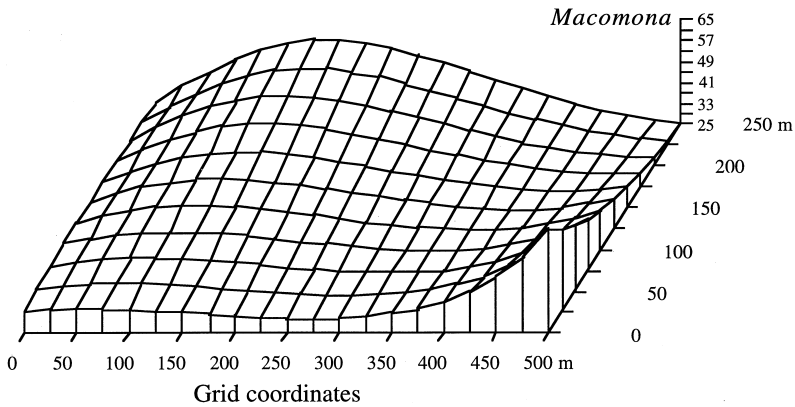
(b) Trend surface map

Fig. 4. *Macomona*>15 mm from 200 sites, 22 January. (a) Actual counts at sampling stations in the 200 regular grid cells; in the field, the stations were not equispaced. (b) Map of the trend surface equation explaining 32% of the spatial variability of the data. The values estimated from the trend-surface equation (log-transformed data) have been back-transformed to raw counts before plotting. The sampling grid is viewed from the south.

3.2. Are the patterns stable through time?

Comparisons between 22 January and 16 February are possible only for large animals (*Macomona*>15 mm, *Austrovenus*>10 mm), because only these variables provide whole-plot counts for both dates, even if only at 31 stations. Paired *t*-tests performed on the normalised (log-transformed: $\ln(x+1)$) data show that there is a slight but highly significant difference in means of the log-transformed data for large *Macomona* (abundances decreased: mean for 22 January in the original count scale=40 animals per quadrat, mean for 16 February=31; for log-transformed data: $t=5.27$, d.f.=30; the difference would remain significant after correction for autocorrelation), but not for large *Austrovenus* (mean for 22 January=1.9 animals per quadrat, mean for 16 February=2.3; for log-transformed data: $t=0.81$, d.f.=30).

(a) *Macomona* 0.5-2.5 mm counts at the 199 sampling stations

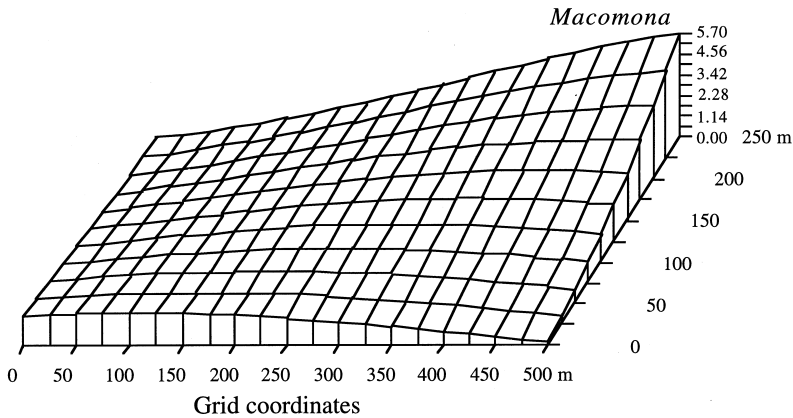| 0	1	0	2	0	1	2	6	2	0	5	1	6	2	2	2	3	6	11	7
0	0	3	1	0	0	4	2	7	2	5	•	8	0	1	7	3	5	6	3
0	0	0	5	5	4	0	6	2	8	8	4	8	3	10	2	6	5	5	5
0	0	0	0	1	5	3	0	0	4	1	0	2	4	3	0	3	5	0	0
4	0	2	3	6	3	7	3	2	3	1	2	3	9	3	1	3	4	3	3
0	10	0	0	0	10	0	0	2	1	0	0	5	2	1	10	4	1	2	0
0	1	0	2	0	4	0	1	0	0	0	11	2	6	8	2	11	0	1	1
2	0	6	3	2	3	1	2	4	0	2	0	8	2	1	12	8	7	5	2
0	4	0	0	5	7	3	0	1	0	1	1	0	1	0	0	0	0	2	0
0	10	6	5	3	5	4	3	0	3	4	6	0	0	0	5	0	6	0	0

(b) Trend surface map

Fig. 5. *Macomona* 0.5–2.5 mm from 199 sites, 22 January. Presentation as in Fig. 3. Dot: missing datum. The trend surface equation explains 15% of the spatial variability of the data.

To assess the consistency of spatial patterns, for the 31 stations that were sampled on two occasions, a spatial pattern of *differences* was determined (Legendre and McArdle, 1997). For both large *Macomona* and large *Austrovenus*, no significant trend surface could be identified among the 31 difference values. So there is no indication of changes *in shape* over the three-week interval. This exercise could not be done for the next size class as data were not available for the same sampling grain (see *Bivalve count data*, Section 2.2).

Correlations between dates were also computed to measure the similarity, or stability of values between dates; differences in mean would not be found by this analysis because correlations are computed on differences from the respective means. Correlations were high for large *Macomona*, between whole-plot counts on 22 January and 16 February ($r = 0.7040$); the same was true for large *Austrovenus* ($r = 0.7050$). So, again, adult counts seem fairly stable across three weeks. Such was not the case for smaller individuals, however; the correlation for *Macomona* 4–15 mm between core counts on

(a) *Austrovenus* counts at the 200 sampling stations

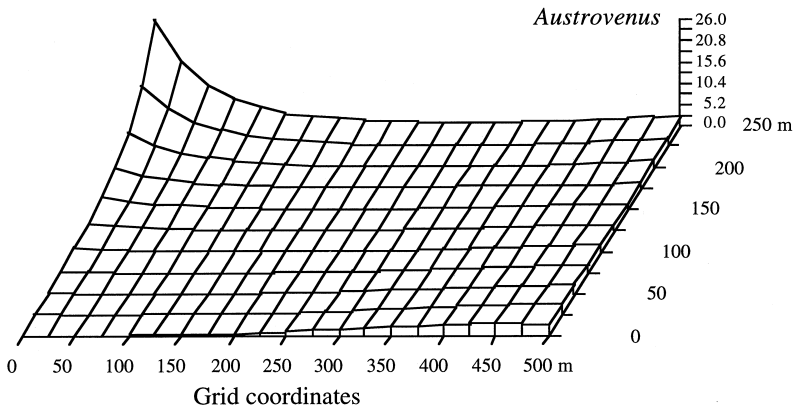|																			
38	11	6	12	1	6	4	3	0	0	1	2	2	8	0	0	1	1	0	2
13	4	6	0	7	2	1	2	0	0	0	1	0	2	1	1	2	34	1	3
9	1	3	0	0	0	2	3	2	1	0	0	0	3	3	0	1	0	0	1
3	4	2	1	0	1	1	2	1	2	0	0	3	0	0	1	0	0	1	3
3	0	1	0	1	0	1	2	2	0	0	2	0	1	1	3	3	2	1	1
2	1	0	4	0	1	0	0	0	1	0	1	1	5	3	11	0	0	5	2
1	0	0	0	0	1	0	0	0	0	0	0	1	1	1	1	0	2	6	0
0	0	0	0	0	0	0	0	0	1	1	0	0	0	0	0	0	4	2	6	1
0	0	1	0	0	1	0	0	0	1	0	3	0	0	3	1	2	1	8	2
0	2	1	0	1	0	0	1	0	2	2	3	0	1	2	2	4	2	3	3

(b) Trend surface map

Fig. 6. *Austrovenus* > 10 mm from 200 sites, 22 January. Presentation as in Fig. 3. The trend surface equation explains 35% of the spatial variability of the data.

22 January and whole-plot counts on 16 February is negative ($r = -0.3055$). This indicates that a change occurred.

3.3. Are the patterns the same across species and size classes?

The principal component analysis (Fig. 8(a)) clearly reveals that large *Macomona* (>15 mm) had similar distributions in the two dates; the same is true for large *Austrovenus* (>10 mm). However, the large *Macomona* behave very differently from the large *Austrovenus*. The same picture was obtained using log-transformed data instead of raw counts.

Drawing arrows from the smaller to the larger size classes of each species, for each sampling date, suggests an interesting relationship (Fig. 8(b–c)). While intermediate-sized *Macomona* (4–15 mm) on 22 January are unrelated to intermediate-sized *Macomona* on 16 February, the large animals are quite highly correlated. Because there were so few *Austrovenus* 4–10 mm in the core samples of 22 January, we don't know

(a) *Austrovenus* 0.5-2.5 mm counts at the 199 sampling stations

```
0   0   0   0   1   1   1   2   0   0   3   1   0   1   5   0   1   1   0   1
0   0   2   1   0   0   2   0   1   0   0   •   0   0   0   0   0   0   1   1
1   1   1   2   1   2   0   2   1   1   2   2   0   0   1   0   0   0   1   3
1   1   0   2   2   1   2   0   3   4   3   0   0   1   0   1   0   0   0   0
3   1   3   4   3   1   0   2   1   1   0   2   1   0   1   0   0   0   0   1
0   9   1   1   0   1   4   0   3   0   0   0   1   0   1   1   0   1   0   1
7   4   1   1   1   3   0   2   0   0   1   2   0   1   2   0   0   0   0   0
3   3   2   1   0   3   0   0   3   0   2   0   1   0   0   1   0   1   0   1
0   2   0   3   0   0   1   0   1   0   0   0   0   2   0   0   1   0   0   0
1   7   1   0   1   0   1   1   1   2   1   1   0   1   0   0   0   2   0   0
```
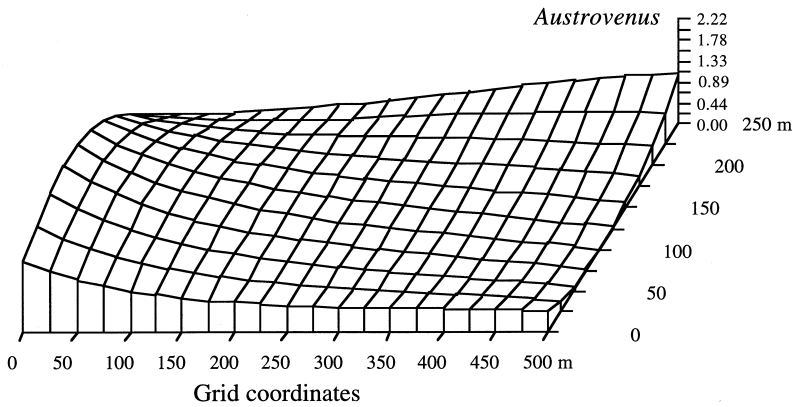
(b) Trend surface map

Fig. 7. *Austrovenus* 0.5–2.5 mm from 199 sites, 22 January. Presentation as in Fig. 3. Dot: missing datum. The trend surface equation explains 17% of the spatial variability of the data.

whether animals pertaining to this size class would be found in the same or different portions of the graph on 22 January and 16 February, although we know that their mean density over the study site changed from 2 to 7 animal·m^{-2} during that time interval. We know, however, that large *Austrovenus* (>10 mm) are clearly found together in the plot on the two dates, in a location opposite to large *Macomona*. In contrast, small animals (<4 mm) of both species are found in the same region of the plane of the first two principal components (lower left in Fig. 8(a)); their correlation is 0.2039.

3.4. Spatial modelling of bivalve counts

A summary of the five-step spatial modelling procedure, for each of the 11 bivalve count variables, is presented in Table 3, with detailed examples in Appendix A. Interpretation will focus on the signs of the significant regression coefficients, summarised in Table 4. Besides the variables found in Table 4, variables from the spatial polynomial turned out to be significant in three models (modelling step 3 in Table 3;
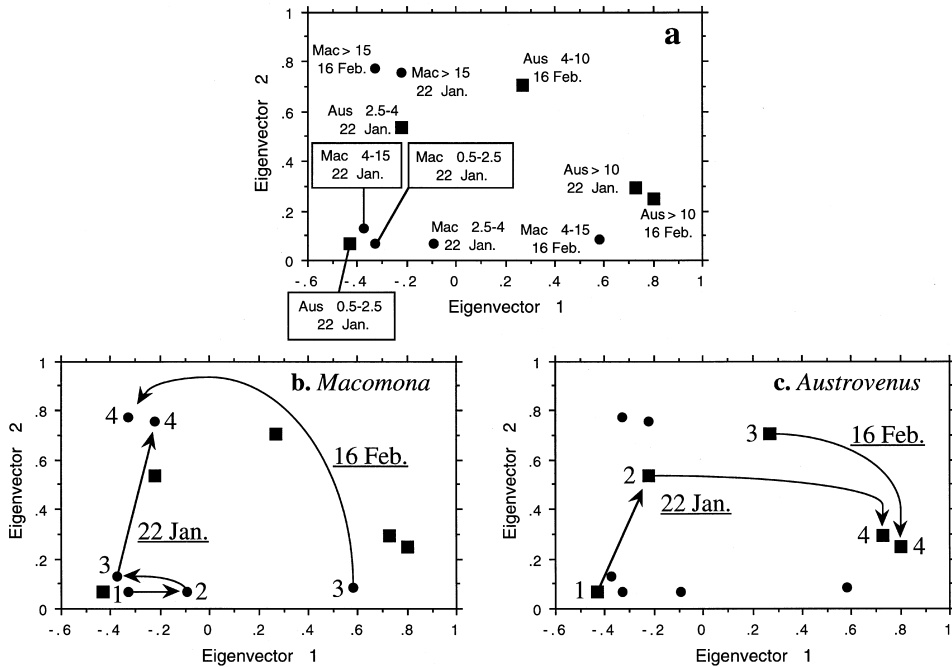
Fig. 8. (a) Bivalve count variables represented in space of the first two eigenvectors, accounting together for 40% of the variation of the correlation matrix (1: 20.4%; 2: 19.6%). *Macomona* is represented by circles, *Austrovenus* by squares. (b) Interpretation of the same graph for *Macomona*. Arrows indicate the size sequence for each sampling date. Size classes are represented by numbers. (c) Same for *Austrovenus*.

only the signs of the significant partial regression coefficients are shown): $-X$, $-XY$ and $+X^3$ for *Macomona* >15 mm, 22 January; $+X^2$ for *Macomona* 4–15 mm, 16 February; $-X^3$ for *Austrovenus* >10 mm, 22 January; $+X^2$ and $-XY$ for *Austrovenus* >10 mm, 16 February.

At the scale of the 250 m $\times$ 500 m study site, the physical variables had significant contributions to the explanation of count variation in all *Macomona* and *Austrovenus* size classes, except *Macomona* (4–15 mm) sampled on 16 February (Table 3). The biological variables explained residual variation in counts in the smallest *Macomona* and *Austrovenus*.

Residual spatial variability, operating at the scale of the study site or larger, was detected in the larger animals. In the largest *Macomona* and *Austrovenus*, for example, spatial terms in X^3 were significant in modelling step 3, indicating the presence of residual spatial variation at the scale of 500 m. Combinations of physical and biological variables explained most of the large-scale spatial structure in bivalve counts (scale of the study site); indeed, there is little or no significant spatial variation left in modelling steps 3 and 5 of Table 3. The unexplained variability (1 minus the R^2 value given in last column of Table 3) can be attributed either to spatially-structured variability at the scale of the study site that cannot be expressed as a linear combination of the terms of the

Table 3
Spatial modelling of the bivalve count variables (dependent variables)

Dependent variable	n	Step 1 Spatial R^2	Step 2 Physics R^2	Step 3 + spatial ΔR^2	Step 4 Physics + biology R^2	ΔR^2	Step 5 + spatial ΔR^2	Total R^2
Macomona								
>15 mm, 22 Jan.	200	0.3171	0.2583*	0.0726*	—	—	—	0.3309
4–15 mm, 22 Jan.	200	0.1192	0.1060*	0.0268ns	—	—	—	0.1060
2.5–4 mm, 22 Jan.	199	0.1094	0.1653*	0.0345ns	—	—	—	0.1653
0.5–2.5 mm, 22 Jan.	199	0.1458	0.2234*	0.0233ns	0.3785*	0.1551*	0.0320ns	0.3785
>15 mm, 16 Feb.	31	0.3936	0.4880*	0.0926ns	—	—	—	0.4880
4–15 mm, 16 Feb.	31	0.1503	—	0.1503*	—	—	—	0.1503
Austrovenus								
>10 mm, 22 Jan.	200	0.3483	0.3421*	0.0186*	—	—	—	0.3606
2.5–4 mm, 22 Jan.	199	0.1617	0.2126*	0.0304ns	—	—	—	0.2126
0.5–2.5 mm, 22 Jan.	199	0.1694	0.1894*	0.0316ns	0.2810*	0.0917*	0.0378ns	0.2810
>10 mm, 16 Feb.	31	0.5508	0.6872*	0.1036*	—	—	—	0.7907
4–10 mm, 16 Feb.	31	0.2917	0.3437*	0.2383ns	—	—	—	0.3437

Step 1 reports the R^2 coefficients of the spatial models in Table 2. Step 2: model using the physical variables only: R^2. Step 3: adding the spatial to the physical variables: ΔR^2 is reported; when a significant spatial polynomial cannot be found, the ΔR^2 is given for all nine terms of the spatial polynomial. Step 4: the physical and biological variables: R^2, ΔR^2. Step 5: adding the spatial to the physical and biological variables: ΔR^2. Total R^2: R^2 value reached using all the significant variables in the models. The significance level is 0.05. R^2 = coefficient of determination; ΔR^2 = increase in R^2 from the model without the stated "+" variables to the model that includes them. * = significant at the 0.05 level; ns = spatial structure not significant; —— = no significant term was found.

cubic trend-surface equation, or to smaller-scale phenomena, since the spatial polynomial of the geographic coordinates X and Y was limited by design to power 3, as explained in Section 2.4; smaller scales have been investigated by Hewitt et al. (1997).

4. Discussion

We have shown (Fig. 2; Figs. 4–7) that the bivalve count variables are spatially structured at the scale of our study site. We expected physical processes to be also spatially structured at that scale, because of the large size of the study site. So, the action of physical variables on bivalve counts, if any, should be detectable at that scale, and could contribute to explain the spatial structure of the bivalve counts, detected by the trend-surface polynomial equations (Table 2).

Our pilot study (Hewitt et al., 1997: cross-correlograms) indicated that interactions between species and size classes of the two dominant bivalves, when they could be detected, were found at scales no larger than 0 to 5 m. Negative adult–juvenile interactions amongst *Macomona* were indicated by the increased flux of juveniles in areas of high adult density (Turner et al., 1997) and were demonstrated in experimental plots throughout the study site (Thrush et al., 1997a). Thus interactions appear to

Table 4
Summary of the significant contributions of the physical and biological variables to the various regression models

	Shell hash	Elevation	Elevation^2	Elevation^3	Ebb stress	Flood stress	SW work	WSW work	>20 cm water	Wave stirring	Macomona 2.5–4 mm	Macomona 0.5–2.5 mm	Austrovenus 2.5–4 mm	Austrovenus 0.5–2.5 mm
Macomona														
>15 mm, 22 Jan.		+	−	+					+					
4–15 mm, 22 Jan.		+				+								
2.5–4 mm, 22 Jan.	−	+				+			+					
0.5–2.5 mm, 22 Jan.	−	+			+	+			+		+		+	+
>15 mm, 16 Feb.		+		+					+					
4–15 mm, 16 Feb.														
Austrovenus														
>10 mm, 22 Jan.		−	+	−		+			−					
2.5–4 mm, 22 Jan.	−	+	−	+	+				+					
0.5–2.5 mm, 22 Jan.		+					−	+	+	−	−	+		
>10 mm, 16 Feb.		−	+	−					−					
4–10 mm, 16 Feb.	−					−								

Signs are the signs of the partial regression coefficients.

function well below the scale of the present study, where the mean distance among neighbouring samples is about 30 m. As a consequence, we do not expect biological interactions between the life stages of the two dominant bivalve species to explain any of the observed large-scale variation; this point is further discussed in Section 4.2. On the other hand, if biological variables are incorporated into models as surrogates for unmeasured physical processes (e.g. localised phenomena not effectively modelled or measured by Bell et al., 1997), they should not create any new large-scale spatial structure in the residuals of the models. This point has been examined (modelling step 5).

4.1. Explaining the spatial structure of bivalve counts

Spatial variation (i.e. the variation explained by the spatial polynomial) is used in the present study simply as an indication of a significant spatial pattern in the dependent variable under study (bivalve count), at the scale of our study site. Such an indication does not contain any interpretation per se. It simply justifies our search for ecologically meaningful hypotheses capable of explaining away the spatially-structured variation of the dependent variable (Borcard and Legendre, 1994). The spatial modelling is considered fully successful when there is no significant spatial variation left to be explained in the data. Admittedly, the technique is limited in that the spatial polynomial used in the present study can only capture the large-scale structures of the dependent variables. Other techniques should be used to model small-scale autocorrelation in the data (Legendre and Borcard, 1994).

Our analyses have shown that there are large-scale spatial structures in all bivalve count variables investigated in this study (Table 2; Table 3, step 1), and that most of these large-scale structures disappear when physical and biological variables are included in models. This result also indicates that our sampling design—25 m resolution within a 250 m by 500 m study site—was appropriate because effects of physical variables were detected on bivalves sampled at that scale.

Significant large-scale spatial variation remained unexplained by our models for large bivalves, even though we had included variables for all of the physical factors commonly evaluated by benthic ecologists. Patterns in the maps of the model residuals (Fig. 9 Fig. 10) may indicate possible explanations for the remaining variation (Borcard and Legendre, 1994). In the present case, the trend surface equations of the residuals indicate that some process, structured as X^3, seems to be at work in both maps, but with effects bearing opposite signs. The nature of that process remains unknown.

The importance of ecological processes (physical or biological) varied for different-sized animals, across a study site chosen to represent basically a flat and homogeneous environment in terms of its major physical characteristics. (a) Larger organisms displayed a significant spatial structure, with physical variables explaining some but not all of this spatial variation. (b) Smaller organisms were less strongly spatially structured; virtually all of their large-scale spatial variation could be explained by physical variables. (c) Regression models for larger organisms include physical variables only, whereas models for the smallest animals include physical variables as well as a few
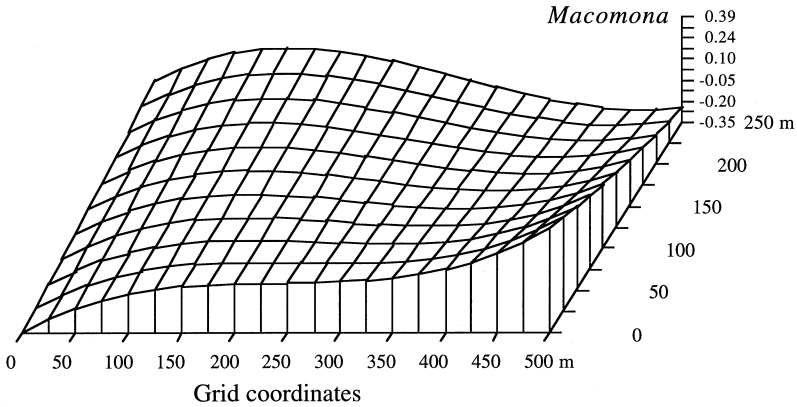
Fig. 9. Map of the spatial component model ($-0.920\,X - 7.914\,XY + 23.854\,X^3$) of *Macomona* >15 mm, 22 January. It corresponds to ΔR^2 in step 3 of Table 3. Compare to Fig. 4.

biological variables (other juveniles). The physical variables that are included in the regression models differ among size classes of a species and between species.

4.2. Biological interactions

Interspecific interactions did not explain any of the spatial variation of the larger bivalves. The smallest size classes only (0.5–2.5 mm) responded significantly to inter- and intraspecific interactions amongst juveniles (Table 4). The significant interactions were positive, except between the smallest *Austrovenus* (0.5–2.5 mm) and slightly larger *Macomona* (2.5–4 mm). No avoidance of adults on the part of juveniles has been detected in these models, after the physical variables had been taken into account.
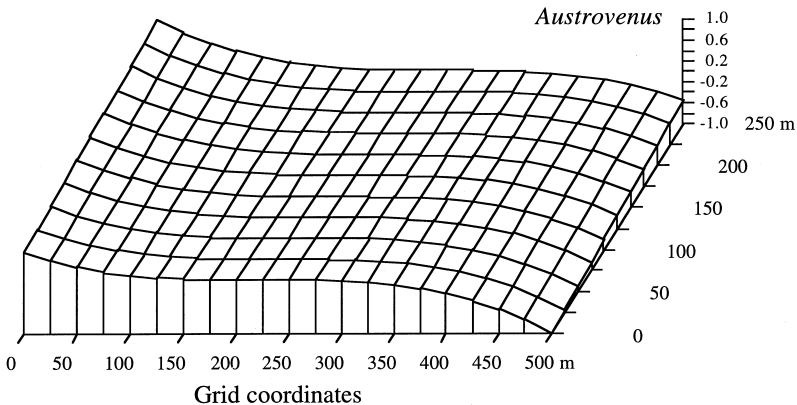

Fig. 10. Map of the spatial component model ($-52.745\,X^3$) of *Austrovenus* >10 mm, 22 January. It corresponds to ΔR^2 in step 3 of Table 3. The slight increase along the $0-250$ m axis is because the sampling grid is not aligned with the easting (X) and northing (Y) geographic coordinates (Fig. 1). Compare to Fig. 6.

Mechanisms for juvenile–juvenile interactions have been documented in some laboratory studies (Ahn et al., 1993), but these relationships may not mean that biological interactions actually took place; they may simply indicate that there were other unmeasured physical variables operating at this small scale, that caused the juveniles to deposit and settle where they were ultimately observed.

4.3. How good are these models?

The fraction of variation explained by the models (Table 3, right-hand column) ranges from 10 to 79%, with a mean value of about 33%. In other words, about 67% of the variation of bivalve counts was not spatially structured or explained by physical variables or interactions with other size classes. The unexplained variability (21 to 90%) found in all models suggests phenomena operating at smaller scales, or variability at the scale of the study site that cannot be expressed as a linear combination of the terms of the cubic trend-surface equation that we used to model large-scale structures, plus a fair amount of Poisson sampling error.

Predation by other species, such as waders (Cummings et al., 1997) and eagle rays (Hines et al., 1997) is a source of variation that we have not examined in this paper. The name of the embayment where this work has been carried out, *Manukau*, is a Maori word meaning ''wading birds'' (X, 1992), by reference to the waders that feed upon bivalves and other invertebrates. There were consistent patterns of variation in usage by shorebirds at the scale of sectors (larger than the study site). Effects at the scale of the study site were expected from previous studies of aggregative responses of shorebirds to natural variation at the scale of 100 m. Contrary to expectation, there were no increases in shorebird numbers or large increases in *Macomona* mortality due to oystercatchers (Cummings et al., 1997). There was no evidence that shorebirds contributed to the unexplained variance by substantially altering spatial variation in prey during the experiment.

It is the extreme size classes (largest and smallest) that were best explained by our models (last column of Table 3). For the largest animals, the physical variables played the most important role. For the 0.5–2.5 mm size classes, biological variables (that may be surrogates for other small-scale physical effects) explained 30 to 40% of the variation accounted for by the models. The patterns displayed by the smaller animals are both different from those of the larger animals, and much less spatially structured (Table 2 and Figs. 4–7).

4.4. The physical variables

Elevation and surrogate variables of hydrodynamic forces played a dominant role in our models. These variables may influence larval deposition, the subsequent transport of juveniles, and food supply. Physical factors together explained from 10% to about 70% of the variation found in the bivalve variables across the Wiroa Island study site. Physical variables derived from hydrodynamic modelling are surrogates for sediment transport, which is responsible for much of the post-larval dispersal. Grant et al. (1997)

clearly demonstrate that sediment transport is spatially and temporally variable. Sediment transport occurs under non-averaged conditions (e.g. high winds) and results from non-linear interaction between waves, tides, and topography.

In nine bivalve models, elevation was significant, sometimes with its square and cubic forms (Table 4); many of the bivalve variables showed significant relationships to a cubic polynomial function of elevation. In most cases, there was a positive partial relationship with elevation, often with a negative relationship with elevation^2 and positive with elevation^3. Elevation controls the action of many of the hydrodynamic variables that, in turn, may be important determinants of the distributions of the various bivalve size classes. The next most important variable, significant in eight models, was the percent of time the plot is covered by more than 20 cm water during spring tide. Even when the effects of the other variables, including elevation, had been controlled for, greater numbers of *Macomona* (all size classes) and *Austrovenus* (0.5–2.5 mm) were found in areas covered by water for longer (Table 4). Large *Austrovenus* (>10 mm) followed the opposite trend.

The ebb and flood shear stress variables measure the transfer of momentum at the sediment interface under peak ebb- and flood-tide velocities during a mean tide. Flood stress made a significant contribution to five models, while ebb stress was significant only in two. Interestingly, Grant et al. (1997) also found more relationships between sediment transport and flood stress than ebb stress. Most size classes of both species were found in greater abundance where flood stress was higher. Small animals tended to avoid locations with higher values of shell hash (Table 4). The mechanism involved is unclear since shell hash is buried below the level where juveniles are found. The distribution of shell hash may be caused by the hydrodynamic processes that also influence the distribution of juveniles.

The SW and WSW wind-work variables were surrogates for work done on the beach by wind-driven waves coming from the predominant wind directions. These variables were only significant for the smallest *Austrovenus* (22 January), where they may be surrogates for other unmeasured variables related to elevation. On 22 January, winds were moderate from the NE, but a 15-knot SW wind had occurred on 19 January. On 16 February, there was a NE breeze up to 15 knots and nothing from the SW. Thus the modelled wind-wave variables do not perfectly reflect the recent history of the site. On any given date, recruits may be deposited on the sediment in a pattern determined by hydrodynamics; changes in the spatial distributions from one time period to another will depend on the species involved (Hewitt et al., in press).

Adults of *Austrovenus*, a facultative suspension feeder, occur in the upper 3 cm of sediment and should be more readily affected by water motion and by physical factors than large *Macomona* which live 7–10 cm below the sediment surface. This is precisely what our regression models have shown (larger R^2 for large *Austrovenus* in step 2 of Table 3).

4.5. Stability of the bivalve distribution patterns

In agreement with the spatial models, principal component analysis suggests that

small *Macomona* and *Austrovenus* (<4 mm) are controlled by similar processes, since they are found in the same region of the plane of the first two principal components. Large *Macomona* and *Austrovenus* (>10 mm) are found in opposite locations, indicating different distributions. Large individuals of each species clearly have the same distribution on both sampling dates, however (Fig. 8(b, c)). The distributions of intermediate-sized animals changed from 22 January to 16 February; *Macomona* (4–15 mm) retained the same mean density over the study site (26 animal·m^{-2}) but changed positions (Fig. 8); conversely, the density of *Austrovenus* (4–10 mm) changed dramatically from 2 to 7 animal·m^{-2}. These findings support the idea that physical processes are controlling the distribution of this size class.

Larger *Macomona* and *Austrovenus* are likely to have lived in the same vicinity for several years, given their restricted mobility as adults. Regardless of how a cohort of bivalves ended up inhabiting a given area, if they have been there for several years, their spatial distribution is a function (likely non-linear) of advection, predation, competition, etc., i.e. all the factors that could impact them over several years. Historical effects make it hard to dissect causative factors post hoc, especially compared to smaller bivalves whose spatial distributions are more likely to bear a close relationship with recent conditions. If those big bivalves arrived at a smaller size (quite likely, given reduced passive movement with size) then they will have gone through the same processes as the smaller ones, but a few years earlier. Thus we are comparing groups of bivalves with different histories. For that reason, the variables that are likely to determine the spatial distribution of larger bivalves in our models are those that remain constant or that represent an integration of physical and biological processes through time, while smaller bivalves are likely to respond to contemporaneous variables. Elevation, with its second and third powers, is the variable that dominates the models for larger animals; it can be seen as an integrated summary of hydrological events over several years.

The potential controlling variables used in this analysis were rarely linearly independent of one another, as is to be expected in any ecological system, and much of the initial effort in developing the spatial models involved variable selection. For the hydrodynamic variables it was necessary to use the results from modelling exercises; this procedure tends to smooth over extreme values that may be ecologically important and emphasise average conditions. We have shown that the spatial variation in different size classes of these bivalves may be related to a variety of ecological processes. The importance of physical or biological processes varied for different-sized animals, across a study site chosen to represent basically a flat and physically homogeneous environment. Our results emphasise the mobility of young bivalves. This mobile post-settlement phase corresponds to sizes<4 mm for *Macomona*, and probably even smaller for *Austrovenus* (Cummings et al., 1995; Commito et al., 1995b). As they grow, their spatial distributions slowly modify to adult patterns. However, in contrast to companion studies (Hewitt et al., 1997; Turner et al., 1997; Thrush et al., 1997a), we found no indication of adult-juvenile interactions *at the scale of our study site*. The use of averaged variables, which may not reflect recent site history, presents difficulties, particularly for the more mobile juvenile bivalves. Larger individuals are less mobile and integrate large-scale extrinsic environmental features over long time periods and are thus more suited to this type of analysis. Variability not explained by the spatial modelling suggests phenomena

operating at different scales, and the limitation of a linear combination of the terms of the trend-surface equations, notwithstanding the influence of random factors, local historical events, and processes operating on different temporal or spatial scales, that may all blur the picture.

Acknowledgements

Appendix A

Two examples of spatial modelling (five steps) are presented to illustrate the process. The first example goes up to step 5 while the second stops at step 4 for lack of significance. Modelling step 1, using the spatial polynomial equation only, is reported in Table 2.

1. *Macomona* 0.5–2.5 mm, 22 January, $n = 199$
   Step 2: Physical variables alone: $R^2 = 0.2234$, $p < 0.0001$. $\hat{y} = -108.860 - 0.069$ Shell hash $+ 23.093$ Elevation $+ 0.044$ Ebb stress $+ 0.688$ Flood stress $+ 107.187$ ''>20 cm water''
   Step 3: Adding the spatial to the physical variables: no term significant. R^2 for 9 terms of spatial polynomial $= 0.24662$; $\Delta R^2 = 0.02325$.
   Step 4: Physical and species variables: attempt to incorporate all the other bivalve counts of 22.01: $R^2 = 0.3785$, $p < 0.0001$; $\Delta R^2 = 0.1551$, partial $F = 14.63917$, $p < 0.0001$. 0.406 ''*Macomona* 2.5–4 mm'' $+ 0.237$ ''*Austrovenus* 2.5–4 mm'' $+ 0.441$ ''*Austrovenus* 0.5–2.5 mm''
   Step 5: Adding the spatial to the physical and biological variables: no term significant. R^2 for 9 terms of spatial polynomial $= 0.41045$; $\Delta R^2 = 0.03199$.
2. *Austrovenus* >10 mm, 16 February, $n = 31$
   Step 2: Physical variables alone: $R^2 = 0.6872$, $p < 0.0001$. $\hat{y} = 7283.651 - 3189.735$ Elevation $+ 856.812$ Elevation$^2 - 122.907$ Elevation$^3 - 6321.219$ ''>20 cm water''
   Step 3: Adding the spatial to the physical variables: $R^2 = 0.7907$, $p < 0.0001$;

$\Delta R^2 = 0.1036$, partial $F = 5.93721$, $p = 0.0080$. Spatial variables (X, Y geographic coordinates) added to the model: $40.725 \ X^2 - 71.248 \ XY$

Step 4: Physical and species variables: attempt to incorporate "*Macomona* > 15 mm" of 16.02 in the equation: not significant.

References

Ahn, I.-Y., Lopez, G., Malouf, R., 1993. Effects of the gem clam *Gemma gemma* on the early post-settlement emigration, growth and survival of the hard clam *Merceneria merceneria*. Mar. Ecol. Prog. Ser. 99, 61–70.

Allen, T.F.H., Starr, T.B., 1982. Hierarchy—Perspectives for Ecological Complexity. University of Chicago Press, Chicago, Illinois, USA, 310 p.

Amanieu, M., Legendre, P., Troussellier, M., Frisoni, G.-F., 1989. Le programme Écothau: théorie écologique et base de la modélisation. Oceanologica Acta 12, 189–199.

Bell, R.G., Hume, T.M., Dolphin, T.J., Green, M.O., Walters, R.A., 1997. Characterisation of physical environmental factors on an intertidal sandflat, Manukau Harbour. New Zealand. J. Exp. Mar. Biol. Ecol. 216 (1–2), 11–31.

Borcard, D., Legendre, P., Drapeau, P., 1992. Partialling out the spatial component of ecological variation. Ecology 73, 1045–1055.

Borcard, D., Legendre, P., 1994. Environmental control and spatial structure in ecological communities: an example using Oribatid mites (Acari Oribatei). Envir. Ecol. Stat. 1, 37–53.

Burrough, P.A., 1987. Spatial aspects of ecological data. In: Jongman, R.H.G., ter Braak, C.J.F., van Tongeren, O.F.R. (Eds.), Data Analysis in Community and Landscape Ecology. Centre for Agricultural Publishing and Documentation (Pudoc), Wageningen, The Netherlands, pp. 213–251.

Butman, C.A., 1987. Larval settlement of soft-sediment invertebrates: The spatial scales of pattern explained by active habitat selection and the emerging role of hydrological processes. Oceanogr. Mar. Biol. Ann. Rev. 25, 113–165.

Cliff, A.D., Ord, J.K., 1981. Spatial Processes: Models and Applications. Pion Limited, London, 266 pp.

Commito, J.A., Currier, C.A., Kane, L.R., Reinsel, K.A., Ulm, I.M., 1995. Dispersal dynamics of the bivalve *Gemma gemma* in a patchy environment. Ecol. Monogr. 65, 1–20.

Commito, J.A., Thrush, S.F., Pridmore, R.D., Hewitt, J.E., Cummings, V.J., 1995. Dispersal dynamics in a wind-driven benthic system. Limnol. Oceanogr. 40, 1513–1518.

Cummings, V.J., Pridmore, R.D., Thrush, S.F., Hewitt, J.E., 1993. Emergence and floating behaviours of post-settlement juveniles of *Macomona liliana* (Bivalvia: Tellinacea). Mar. Behav. Physiol. 24, 25–32.

Cummings, V.J., Pridmore, R.D., Thrush, S.F., Hewitt, J.E., 1995. Post-settlement movement by intertidal benthic macroinvertebrates: do common New Zealand species drift in the water column? N.Z. J. Mar. Freshwat. Res. 29, 59–67.

Cummings, V.J., Schneider, D.C., Wilkinson, M.R., 1997. Multiscale experimental analysis of aggregative responses of mobile predators to infaunal prey. J. Exp. Mar. Biol. Ecol. 216 (1–2), 211–227.

Dutilleul, P., Legendre, P., 1993. Spatial heterogeneity against heteroscedasticity: an ecological paradigm versus a statistical concept. Oikos 66, 152–171.

Emerson, C.W., Grant, J., 1992. The control of soft-shell clam (*Mya arenaria*) recruitment on intertidal sandflats by bedload sediment transport. Limnol. Oceanogr. 36, 1288–1300.

Ertman, S.C., Jumars, P.A., 1988. Effects of bivalve siphonal currents on the settlement of inert particles and larvae. J. Mar. Res. 46, 797–813.

Grant, J., Turner, S.J., Legendre, P., Hume, T.M., Bell, R.G., 1997. Patterns of sediment reworking and transport over small spatial scales on an intertidal sandflat, Manukau Harbour. New Zealand. J. Exp. Mar. Biol. Ecol. 216 (1–2), 33–50.

Grant, W.D., Madsen, O.S., 1979. Combined wave and current interaction with a rough bottom. J. Geophys. Res. 84, 1797–1808.

Haining, R., 1990. Spatial Data Analysis in the Social and Environmental Sciences. Cambridge University Press, Cambridge, xxi + 409 pp.

Haury, L.R., McGowan, J.A., Wiebe, P.H., 1978. Patterns and processes in the time-space scales of plankton distributions. In: Steele, J.H. (Eds.), Spatial Pattern in Plankton Communities. Plenum Press, New York, pp. 277–327.

He, F., Legendre, P., Bellehumeur, C., LaFrankie, J.V., 1994. Diversity pattern and spatial scale: a study of a tropical rain forest of Malaysia. Envir. Ecol. Stat. 1, 265–286.

Hewitt, J.E., Pridmore, R.D., Thrush, S.F., Cummings, V.J., in press. Assessing the short-term variability of spatial patterns of macrobenthos in a dynamic estuarine system. Limnol. Oceanogr.

Hewitt, J.E., Legendre, P., McArdle, B.H., Thrush, S.F., Bellehumeur, C., Lawrie, S.M., 1997. Identifying relationships between adult and juvenile bivalves at different spatial scales. J. Exp. Mar. Biol. Ecol. 216 (1–2), 77–98.

Hines, A.H., Whitlatch, R.B., Thrush, S.F., Hewitt, J.E., Cummings, V.J., Dayton, P.K., Legendre, P., 1997. Nonlinear foraging response of a large marine predator to benthic prey: eagle ray pits and bivalves in a New Zealand sandflat. J. Exp. Mar. Biol. Ecol. 216 (1–2), 191–210.

Isaaks, E.H., Srivastava, R.M., 1989. Applied Geostatistics. Oxford University Press, New York, xix + 561 pp.

Legendre, L., Legendre, P., 1983. Numerical Ecology. Elsevier Scientific Publ. Co., Amsterdam, The Netherlands, xvi + 419 pp.

Legendre, P., 1990. Quantitative methods and biogeographic analysis. In: Garbary, D.J., South, R.G. (Eds.), Evolutionary Biogeography of the Marine Algae of the North Atlantic. NATO ASI Series, G 22, Springer–Verlag, Berlin, pp. 9–34.

Legendre, P., Fortin, M.-J., 1989. Spatial pattern and ecological analysis. Vegetatio 80, 107–138.

Legendre, P., Borcard, D., 1994. Rejoinder. Envir. Ecol. Stat. 1, 57–61.

Legendre, P., Legendre, L., 1997. Numerical Ecology, 2nd English ed. Elsevier, Oxford.

Legendre, P., McArdle, B.H., 1997. Comparison of surfaces. Oceanologica Acta 20, 27–41.

Luckenbach, M.W., 1984. Settlement and early post-settlement survival in the recruitment of *Mulinia lateralis* (Bivalvia). Mar. Ecol. Prog. Ser. 17, 245–250.

Monismith, S.G., Koseff, J.R., Thompson, J.K., O'Riordan, C.A., Nepf, H.M., 1990. A study of model bivalve siphonal currents. Limnol. Oceanogr. 35, 680–696.

Oden, N.L., 1984. Assessing the significance of a spatial correlogram. Geographical Analysis 16, 1–16.

O'Riordan, C.A., Monismith, S.G., Koseff, J.R., 1993. A study of concentration boundary-layer formation over a bed of model bivalves. Limnol. Oceanogr. 38, 1712–1729.

Ripley, B.D, 1981. Spatial Statistics. John Wiley and Sons, New York, x + 252 pp.

Roegner, C., Andre, A., Lindegarth, M., Eckman, J.E., Grant, J., 1995. Transport of recently settled soft-shell clams (*Mya arenaria* L.) in laboratory flume flow. J. Exp. Mar. Biol. Ecol. 187, 13–26.

Schneider, D.C., 1987. Patch structure of benthic populations on an intertidal sandflat. Oceanologica Acta 10, 469–473.

Schneider, D.C., 1994. Quantitative Ecology: Spatial and Temoral Scaling. Academic Press, San Diego, xv + 395 pp.

Snelgrove, P.V.R., 1994. Hydrodynamic enhancement of invertebrate larval settlement in microdepositional environments: colonization tray experiments in a muddy habitat. J. Exp. Mar. Biol. Ecol. 176, 149–166.

Snelgrove, P.V.R., Butman, C.A., 1994. Animal–sediment relationships revisited: cause versus effect. Oceanogr. Mar. Biol. Ann. Rev. 32, 111–177.

Sokal, R.R., Oden, N.L., 1978. Spatial autocorrelation in biology. 1. Methodology. Biol. J. Linnean Soc. 10, 199–228.

Stommel, H., 1963. Varieties of oceanographic experience. Science 139, 572–576.

Student [W.S. Gosset], 1914. The elimination of spurious correlation due to position in time and space, Biometrika, 10, 179–180.

Thrush, S.F., Pridmore, R.D., Hewitt, J.E., Cummings, V.J., 1992. Adult infauna as facilitators of colonization on intertidal sandflats. J. Exp. Mar. Biol. Ecol. 159, 253–265.

Thrush, S.F., Pridmore, R.D., Hewitt, J.E., Cummings, V.J., 1994. The importance of predators on a sandflat: interplay between seasonal changes in prey densities and predator effects. Mar. Ecol. Prog. Ser. 107, 211–222.

Thrush, S.F., Hewitt, J.E., Pridmore, R.D., Cummings, V.J., 1996. Adult/juvenile interactions of infaunal bivalves: contrasting outcomes in different habitats. Mar. Ecol. Prog. Ser. 132, 83–92.

Thrush, S.F., Pridmore, R.D., Bell, R.G., Cummings, V.J., Dayton, P.K., Ford, R., Grant, J., Hewitt, J.E., Hines, A.H., Hume, T.M., Lawrie, S.M., Legendre, P., McArdle, B.H., Morrisey, D., Schneider, D.C., Turner, S.J., Walters, R., Whitlatch, R.B., Wilkinson, M.R., 1997a. The sandflat habitat: scaling from experiments to conclusions. J. Exp. Mar. Biol. Ecol. 216 (1–2), 1–9.

Thrush, S.F., Cummings, V.J., Dayton, P.K., Ford, R., Grant, J., Hewitt, J.E., Hines, A.H., Lawrie, S.M., Legendre, P., McArdle, B.H., Pridmore, R.D., Schneider, D.C., Turner, S.J., Whitlatch, R.B., Wilkinson, M.R., 1997b. Matching the outcome of small-scale density manipulation experiments with larger scale patterns: an example of bivalve adult/juvenile interactions. J. Exp. Mar. Biol. Ecol. 216 (1–2), 153–169.

Turner, S.J., Grant, J., Pridmore, R.D., Hewitt, J.E., Wilkinson, M.R., Hume, T.M., Morrisey, D.J., 1997. Bedload and water-column transport and colonization processes by mobile post-settlement benthic macrofauna: Does infaunal density matter? J. Exp. Mar. Biol. Ecol. 216 (1–2), 51–76.

Upton, G., Fingleton, B., 1985. Spatial Data Analysis by Example. Vol. 1: Point Pattern and Quantitative data. John Wiley and Sons, Chichester, xi+409 p.

X, 1992. Maori Place Names, Their Origins and Meanings. Reed Books, Auckland, 95 pp.